

# A new translating quasigeostrophic V-state

N. Robb McDonald

*Department of Mathematics, University College London, Gower Street, London WC1E 6BT, UK*

Received 4 June 2003; received in revised form 13 October 2003; accepted 27 October 2003

Available online 20 December 2003

---

## Abstract

A new nonlinear translating V-state of the barotropic quasigeostrophic equations with topography in the form of an infinitely long escarpment (or step) is computed numerically. Before the numerical computation, with the assumption of small excursions by fluid columns across the step, the linear equations of motion are solved analytically, demonstrating the possibility of constructing a translating V-state. The linear V-state has zero total circulation and self-propagates parallel to the step. It consists of two line vortices with positive circulation located on the deep side of the step and a finite-area patch of constant negative vorticity on the shallow side comprising of fluid which has crossed the step from the deep side. The linear solution motivates the numerical search for a nonlinear translating V-state comprising of two line vortices and a finite-area patch of constant vorticity. An algorithm based on contour dynamics and Newton's method is used to find such a V-state. Time-dependent contour dynamics is used to compute the evolution of the V-state and it is found to be unstable. However, the growth rate of disturbances is sufficiently small for the V-state to survive several turn-over times.

© 2003 Elsevier SAS. All rights reserved.

*Keywords:* Vortex dynamics; Geophysical fluid dynamics

---

## 1. Introduction

Two-dimensional distributions of vorticity which either translate or rotate without change of shape have been the subject of much attention in the literature. Such configurations of vorticity represent exact solutions of the two-dimensional Euler equations (or their dynamical equivalent, the barotropic quasigeostrophic equations) and have been given the names of V-states or vortex crystals. The simplest such V-states involve relatively few numbers of line vortices. For example, two line vortices with equal but oppositely signed circulation translate in a straight line at constant speed. If, on the other hand, the circulations are of the same sign, the vortices rotate about each other with constant angular velocity. Aref et al. [1] give details on many other vortex crystals consisting of multiple line vortices in not only planar geometry, but other two-dimensional manifolds such as, for example, the surface of a sphere.

V-states comprising of finite-area patches of constant vorticity have been computed numerically by several researchers. The advantage of considering constant vorticity, rather than more general continuous distributions of vorticity, is that the velocity field everywhere is determined by the shape of vortex boundary, and thus the numerical task is considerably simplified. Indeed the computation of V-states was one of the original uses of the now well-established numerical method contour dynamics. For example, Deem and Zabusky [2] and, later, Wu, Overman and Zabusky [3] computed the shapes of rotating and translating V-states. Pierrehumbert [4] also computed numerically the shape of a pair of finite-area patches with equal but opposite constant vorticity in steady translation.

Recently, Crowdy [5–7] in a series of papers has used analytical methods based on the theory of Schwarz functions to construct exact solutions to the Euler equations which are in steady rotation (with possibly zero angular velocity).

---

*E-mail address:* [robb@math.ucl.ac.uk](mailto:robb@math.ucl.ac.uk) (N.R. McDonald).

A characteristic feature of his solutions is they consist of finite-area patches of constant vorticity together with a finite number of line vortices.

Other steady translating vorticity distributions can be constructed by special choices of the vorticity distribution. For example, the well-known Lamb dipole is a steadily translating exact solution of the two-dimensional Euler equations consisting of a circular patch of continuously varying vorticity such that the vorticity is a linear function of the streamfunction (for a history of this solution see Meleshko and van Heijst [8]). Similar solutions have been constructed for the quasigeostrophic equations on the  $\beta$ -plane where they are known as modons-see, e.g., Flierl et al. [9].

The aim here is to compute a translating V-state of the barotropic quasigeostrophic equations incorporating topography in the form of an infinitely long escarpment or step. Such a choice of topography ensures that the distribution of vorticity owing to the displacement of fluid columns across the escarpment will always be piecewise constant. In particular, potential vorticity conservation demands that fluid columns which cross the step acquire positive or negative relative vorticity of an amount proportional to the change in depth. Moreover, escarpment topography is of relevance to the propagation of ocean vortices and has been previously used by Dunn, McDonald and Johnson [10] to investigate the time-dependent motion of vortices near topography. Given the present task of constructing steady solutions, a complicating feature of the step topography is that it acts as wave guide and that, in general, a vortex will radiate topographic waves as it moves. Such wave radiation with its associated energy loss and wave drag must result in unsteady vortex motion. Note also that the barotropic quasigeostrophic equations with step topography are dynamically equivalent to the two-dimensional Euler equations with a piecewise constant shear velocity playing the analogous role of topography in providing a jump in the background vorticity distribution (see, e.g., Bell [11]).

Since the focus here is on constructing steady solutions, a necessary requirement of any solution is to eliminate topographic wave radiation. In a related problem McDonald [12] does this by considering a cylinder of finite radius with circulation. In the linear limit valid for small excursions of fluid columns across the step the effect of the cylinder and circulation can be represented as the superposition of a dipole and a line vortex. For a given cylinder radius, it was shown that there exists a unique value of the circulation such that the downstream wake vanishes. Nonlinear waveless solutions were also found numerically. In contrast to McDonald [12], in the present work the downstream wake is made to vanish by considering two line vortices. Effectively both vortices act as wavemakers, but are placed such that the wakes destructively interfere downstream. The scenario is similar to Tuck and Scullen [13] who showed that in the flow past two cylinders submerged below a free surface it was possible to place them (in both linear and nonlinear cases) such that not only did the downstream wake vanish, but also the force on each cylinder vanished.

A description of the flow problem and governing equations is given in Section 2. In Section 3 linear theory is used to demonstrate the feasibility of constructing a translating V-state comprising of two line vortices and a finite area region of constant vorticity. However, as will be seen, the linear solution also suggests that such a V-state is likely to be nonlinear owing to the order-one amplitude of the displacement of the contour across the step. Section 4 describes a numerical method based on Newton's method, which uses contour dynamics to calculate the velocity field, used to compute the nonlinear translating V-state. In Section 5 the nonlinear evolution of the V-state is studied using time-dependent contour dynamics and it is shown that the V-state is unstable, but is able to survive several turn-over times. Conclusions are presented in Section 6.

## 2. Description of the flow problem

The flow of barotropic, rotating fluid according to quasigeostrophic dynamics is governed by the conservation of potential vorticity  $q^*$ , i.e.,

$$q^* = \nabla^2 \psi^* + q_0^*, \quad (1)$$

where  $\psi^*$  is a streamfunction and  $q_0^*$  is the background potential vorticity. In this problem the background potential vorticity is given by  $q_0^* = \omega^* H(y^*)$ , where  $H(y^*)$  is the Heaviside step function. Here the jump in potential vorticity  $\omega^*$  is owing to topography in the form of an infinitely long escarpment which separates fluid of shallow depth ( $y > 0$ ) from fluid of deep depth ( $y < 0$ ). Though not considered here, an alternative way of achieving a similar distribution of potential vorticity in a fluid of uniform depth would be to consider a background shear flow with piecewise constant vorticity.

It is known from the study of Dunn et al. [10] that a cyclonic vortex located on the deep side of the escarpment will tend to propagate parallel to the escarpment with shallow water on its right. Earlier, McDonald [14] showed that sufficiently intense vortices of either circulation will propagate with shallow water on their right. This is in keeping with the well-known tendency of geophysical vortices to propagate with regions of high potential vorticity on their right, e.g., the 'westward' propagation of vortices on the  $\beta$ -plane. Hence the present work concentrates on vortices which propagate to the left, or equivalently, stationary vortices embedded in a uniform flow toward positive  $x$ . This (as opposed to vortices which propagate to the right) is the more challenging problem since in this situation topographic waves are excited (see later) leaving a wavetrain behind the vortex. Obviously, owing to non-zero wave drag on the vortices, such a (radiating) situation cannot ever be steady. In this problem two cyclonic vortices each with positive circulation  $\Gamma^*$  (with magnitude to be determined) are assumed to lay in deep water (i.e.,

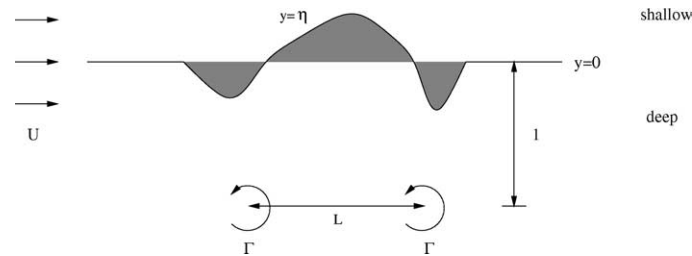


Fig. 1. The non-dimensional flow problem. The shaded areas bounded by the curve  $y = \eta$  and  $y = 0$  are regions of non-zero relative vorticity which arise from fluid crossing the step. Fluid going from deep to shallow water (i.e., the shaded region  $y > 0$ ) acquires relative vorticity of  $-1$ . Similarly, fluid crossing the step from shallow to deep water (i.e., the shaded region  $y < 0$ ) acquires relative vorticity of  $+1$ .

$y < 0$ ) equidistant from the escarpment and propagate steadily with speed  $U^*$  (also to be determined) in a direction such that shallow water lies on their right. For two vortices it will be shown that it is possible, at least according to linear theory, such that their combined wake vanishes downstream, this being a necessary (but not sufficient) condition for a steadily translating solution. It is also emphasised that the solution sought is to be self-propagating. That is, it is the mutual self-advection of the vorticity distribution itself that drives the translation; no artificial propagation mechanism is imposed.

Following McDonald [12] the equations of motion are non-dimensionalised using the distance of the vortices from the escarpment as the lengthscale and  $\omega^*$  as the timescale. The resulting non-dimensional flow problem is shown in Fig. 1 in a frame such that the vortices are fixed. The non-dimensional parameters are the horizontal separation distance of the vortices  $L$ , the upstream flow speed  $U$  and the circulation of the vortices  $\Gamma$ .

Viewed as an initial value problem, after the flow has been initiated, the presence of the vortices causes fluid columns to cross the isobath. As they do so, potential vorticity conservation demands that they acquire relative vorticity. In particular, fluid columns crossing from deep to shallow water acquire negative relative vorticity, i.e.,  $\nabla^2 \psi = -1$ ; and those crossing from shallow to deep water acquire positive relative vorticity, i.e.,  $\nabla^2 \psi = 1$ . As shown in Fig. 1, the region of fluid on the shallow side of the step, which has acquired negative vorticity, circulates clockwise as indicated by the dashed arrow. For problems of the type here which involve piecewise constant distributions of vorticity, the velocity field at any point of the fluid is determined by the location of the contour. The velocity field, in turn, affects the displacement of the contour, leading, in general, to a complex, nonlinear evolution of the contour.

The aim here is to find *steady* solutions for the contour displacement  $y = \eta(x)$ , which satisfy a nonlinear boundary condition at  $y = \eta(x)$ , and such that the velocity at the centre of each of the vortices vanishes, i.e., they remain fixed. This is a difficult nonlinear boundary value problem which (seemingly) must be tackled numerically. However in the linear limit, valid for small amplitude  $\eta(x)$ , it is shown in the next section that a steady solution is possible.

### 3. The linearized problem

As in McDonald [12] it is useful to discuss briefly the properties of the free topographic waves before considering the linear version of the flow problem depicted in Fig. 1.

#### 3.1. Free waves

The conservation of potential vorticity provides a restoring force resulting in wave propagation. In the present problem, the dispersion relation for the waves in a free stream of speed  $U$  is (e.g., Bell [11])

$$\sigma = Uk - \frac{\text{sgn} k}{2}, \quad (2)$$

where  $\sigma$  is the frequency and  $k$  the wavenumber. The phase and group velocities are

$$c_p = U - \frac{1}{2|k|}, \quad c_g = U - \delta(k), \quad (3a,b)$$

where  $\delta$  is the delta function. Note, in the absence of the stream  $U$ , the phase velocity of the waves is negative for all wave numbers. That is the waves propagate toward decreasing  $x$  with high values of potential vorticity (shallow water) on their right looking in the direction they propagate. Such preferential direction of phase propagation is typical of vorticity waves.

Steady waves can form in the lee of the vortices provided  $c_p = 0$ , i.e., from (3a), when

$$U = \frac{1}{2|k|}, \quad (4)$$

which is satisfied for some  $|k|$  for all  $U > 0$ . Thus for any positive upstream velocity, the flow will be accompanied by a wake in the lee of the vortices with wavenumber  $k = 1/2U$ . For negative upstream velocities  $U$  condition (4) cannot be satisfied and no steady wake is possible. This corresponds to fluid flowing toward negative values of  $x$  or, in a fixed frame, vortices which propagate toward positive  $x$ . As argued earlier this is a geophysically less relevant case than the  $U > 0$  case (when a wake is possible) considered here. Bell [11] discusses various cases for the initial value problem of suddenly initiating a flow past a single vortex including quasi-steady solutions with downstream wakes. The ‘quasi’ referring to the fact that owing to wave radiation of small amplitude waves the solution is not truly steady and does evolve over long timescales.

### 3.2. The linear solution

Here, only the case  $U > 0$  is considered, i.e., when, in general, a downstream wake occurs in the lee of the vortices. Since the task is to find steadily propagating solutions it is necessary to find non-radiating solutions. In this section, linear theory is used to construct a non-radiating solution by considering two vortices which are appropriately placed so that their individual downstream wakes destructively interfere, and such that the velocity at the vortices vanish so that they remain stationary. In a frame of reference such that fluid at infinity is quiescent, such a solution represents a vorticity distribution which translates steadily toward negative  $x$ .

Following McDonald [12], the linear problem is to find  $y = \eta(x)$ ,  $|\eta| \ll 1$ , by solving

$$U \frac{d\eta}{dx} = v, \quad \text{on } y = 0, \quad (5)$$

where

$$v = \frac{d}{dx} \left\{ -\frac{1}{2\pi} \int_{-\infty}^{\infty} \int_0^{\eta(x')} \log \left[ ((x-x')^2 + (y-y')^2)^{1/2} \right] dy' dx' + \frac{\Gamma}{2\pi} (\log r_- + \log r_+) \right\}, \quad (6)$$

where  $r_{\pm}^2 = (x \pm L/2)^2 + (y + 1)^2$ . In writing (6) it has been assumed that the line vortices have the same circulation  $\Gamma$ , are both unit distance from the escarpment and separated horizontally by a distance  $L$ . The area integral term inside the brackets on the right-hand side of (6) represents the streamfunction owing to the relative vorticity induced by the displacement of the contour. The solution of (5) is to be found subject to a radiation condition, namely that no waves occur upstream of the vortices.

Consistent with linear dynamics the approximations  $|\eta| \ll 1$  and  $y = 0$  are made in (6) and Fourier transform of (5) and (6) subsequently gives

$$U i k \bar{\eta} = \frac{i}{2} \operatorname{sgn} k \bar{\eta} - \frac{\Gamma i}{4\pi} \operatorname{sgn} k e^{-|k|} (e^{-ikL/2} + e^{ikL/2}), \quad (7)$$

where

$$\bar{\eta} = \frac{1}{2\pi} \int_{-\infty}^{\infty} \eta e^{-ikx} dx. \quad (8)$$

Solving (7) for  $\bar{\eta}$  gives

$$\bar{\eta} = -\frac{\Gamma}{2\pi} \operatorname{sgn} k e^{-|k|} \frac{\cos(kL/2)}{kU - (\operatorname{sgn} k/2)}. \quad (9)$$

As argued previously, a steady wave-train appears downstream if condition (4) is satisfied. Inspection of the right-hand side of (9), reveals that this is precisely the condition for  $\bar{\eta}$  to have a simple pole at  $k = 1/2U$ . The contribution of this pole to the Fourier inversion integral for  $\eta$  (deforming the integration contour about the pole in the complex plane to take into account the radiation condition) gives a steady sinusoidal wave train downstream of the vortices. It is crucial to this work to note that for the special choice  $L/2U = (2n+1)\pi$ ,  $n = 0, 1, 2, \dots$ , implies that when  $k = 1/2U$  there is no singularity (and hence no downstream wake occurs) since in (9)

$$\lim_{k \rightarrow 1/2U} \frac{\cos[kU(2n+1)\pi]}{kU - 1/2} = (-1)^{n+1} (2n+1)\pi, \quad n = 0, 1, 2, \dots \quad (10)$$

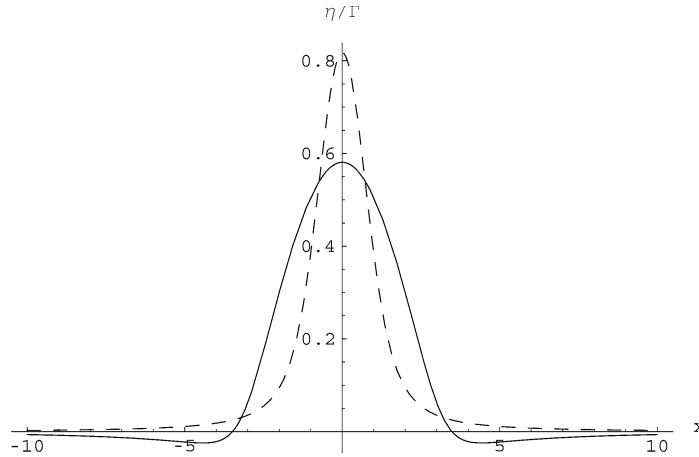


Fig. 2. Profiles of  $\eta(x)$  (normalised by  $\Gamma$ ) with the non-radiating condition  $L = 2\pi U$ ;  $U = 1$  (solid line) and  $U = U_s \approx 0.3023$  (dashed line).

Physically this choice corresponds to two linear wavemakers arranged so that their sinusoidal wakes destructively interfere downstream. For simplicity, in what follows the choice  $n = 0$  is made, i.e., the case when the vortices are closest together. Hence for the non-radiating case  $L = 2\pi U$ , the contour displacement is obtained by inverting the Fourier transform (9) giving

$$\eta(x) = -\frac{\Gamma}{2U\pi} \int_{-\infty}^{\infty} \frac{\operatorname{sgn} k e^{-|k|} \cos kU\pi}{k - (\operatorname{sgn} k)/(2U)} e^{ikx} dk = -\frac{\Gamma}{U\pi} \int_0^{\infty} \frac{e^{-k} \cos kU\pi}{k - 1/(2U)} \cos kx dk. \quad (11)$$

It is clear from (11) that  $\eta(x)$  is even in  $x$  and, up to a scaling parameter  $\Gamma$ , depends only on  $U$ . Fig. 2 shows plots of  $\eta(x)/\Gamma$  obtained by numerical evaluation of (11) for two different choices of  $U$ .

The symmetry of the contour about  $x = 0$  means that the velocity in the  $x$ -direction induced by the vortex patch bounded by the displaced contour is the same for both vortices. Moreover, at least for the two examples shown in Fig. 2, the displacement of the contour is predominantly toward positive  $y$  and this implies that the negative (clockwise) circulation associated with the displaced contour will be dominant and acts to induce a negative velocity in the  $x$ -direction for both vortices (as in the schematic Fig. 1). On the other hand the velocity in the  $y$ -direction induced by the patch is of the same magnitude for both vortices but is negative for the right-hand vortex and positive for the left-hand vortex. In the linear limit the velocity in the  $y$ -direction felt at the vortices due to the vortex patch is, for general  $\eta(x)$ ,

$$v(\pm L/2, -1) = -\frac{1}{2\pi} \int_{-\infty}^{\infty} \frac{\eta(x')(\pm L/2 - x')}{(\pm L/2 - x')^2 + 1} dx'. \quad (12)$$

Substituting (11) in (12) and using the non-radiating condition  $L = 2\pi U$  gives

$$\begin{aligned} v(\pm L/2, -1) &= \frac{\Gamma}{4\pi^2 U} \int_{-\infty}^{\infty} \int_{-\infty}^{\infty} \frac{\operatorname{sgn} k e^{-|k|} \cos(kU\pi)}{k - (\operatorname{sgn} k)/(2U)} e^{ikx'} \frac{(\pm L/2 - x')}{(\pm L/2 - x')^2 + 1} dx' dk \\ &= \pm \frac{\Gamma}{2\pi U} \int_0^{\infty} \frac{e^{-2k}}{k - 1/2U} \cos(kU\pi) \sin\left(\frac{kL}{2}\right) dk = \pm \frac{\Gamma}{4\pi U} \int_0^{\infty} \frac{e^{-2k}}{k - 1/2U} \sin(2\pi U k) dk = \pm v(U). \end{aligned} \quad (13)$$

A plot of  $-v(U)/\Gamma$ ,  $0.1 \leq U \leq 1$ , is shown as the solid line in Fig. 3. Since, for  $\Gamma > 0$ ,  $v(U) < 0$  it follows from (13) that  $v(L/2, -1) < 0$  and  $v(-L/2, -1) > 0$ , i.e., the contour induces a negative velocity in the  $y$ -direction at the right-hand vortex and a positive velocity in the  $y$ -direction at the left-hand vortex. The directions of these velocities is consistent with the negative vorticity associated with the fluid bounded by the contour being deflected toward positive  $y$  – see Fig. 1.

In addition to the velocity induced by the patch of vorticity, each vortex induces a velocity on the other in the  $y$ -direction. In particular, for positive  $\Gamma$  as in Fig. 1, the left-hand vortex advects the right-hand vortex toward positive  $y$  and the right-hand vortex advects the left-hand vortex toward negative  $y$ . Significantly the direction of these vortex-vortex induced velocities is opposite to those induced by the vortex patch and thus it may be possible, by careful choice of parameters, to balance the two opposed velocities so that the velocity in the  $y$ -direction at each vortex vanishes – this being a necessary condition for a

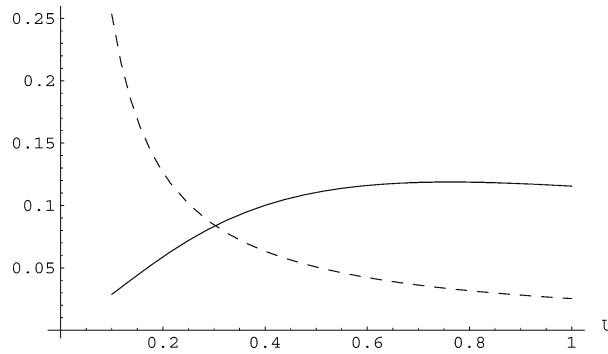


Fig. 3. The curves of  $-v(U)/\Gamma$  (solid line) and  $(4\pi^2 U)^{-1}$  (dashed line). They intersect when  $U = U_s \approx 0.3023$ .

steady solution. The magnitude of the vortex-vortex induced velocities is  $\Gamma/2\pi L$  or  $\Gamma/4\pi U^2$  when the non-radiating condition  $L = 2\pi U$  is chosen. Hence when the condition

$$v(U) + \frac{\Gamma}{4\pi^2 U} = 0, \quad (14)$$

is satisfied the velocity in the  $y$ -direction vanishes at each vortex. Since  $v(U)$  is proportional to  $\Gamma$ , the condition (14) is independent of  $\Gamma$ . Fig. 3 shows plots of  $-v(U)/\Gamma$  obtained by numerical evaluation of (13) and  $(4\pi^2 U)^{-1}$ . Condition (14) is satisfied when the two curves cross, which occurs, to four significant figures, at  $U = U_s \approx 0.3023$ . Fig. 2 show a plot of  $\eta(x)$  (scaled by  $\Gamma$ ) for the choice  $U = U_s$ .

The above demonstrates that it is possible to choose  $U$  (and hence  $L$ , since  $L = 2\pi U$ ) such that the velocity of both vortices in the  $y$ -direction vanishes and the vortex pair is non-radiating. However, it is further required that the  $x$ -velocity of each vortex also vanish. Given that  $U = U_s$  and hence  $L$  are now fixed by the above requirement that the velocity in the  $y$ -direction vanish, the only remaining free parameter is  $\Gamma$ . Proceeding as before, an expression for the velocity in the  $x$ -direction due to the displaced contour with  $U = U_s$  is

$$u(\pm L/2, -1) = -\frac{1}{2\pi} \int_{-\infty}^{\infty} \frac{\eta(x')}{(\pm L/2 - x')^2 + 1} dx' = \frac{\Gamma}{2\pi U_s} \int_0^{\infty} \frac{e^{-2k}}{k - 1/2U_s} \cos^2(\pi U_s k) dk \approx -0.1537\Gamma. \quad (15)$$

Thus in order for the vortices to be stationary it is further required that  $-0.1537\Gamma + U_s \approx 0$  or  $\Gamma = \Gamma_s \approx 1.966$ .

It is encouraging that according to linear theory it is possible to find a steadily translating solution in which both vortices remain fixed in the translating frame. Once the choice is made that the vortices have the smallest possible separation in the  $x$ -direction (i.e.,  $L = 2\pi U$ ) the solution is unique. That is, by demanding that vortices be stationary and the solution be non-radiating, all three parameters  $U$ ,  $L$  and  $\Gamma$  are uniquely determined (these unique values being denoted with the subscript  $s$ ). In a frame of reference such that fluid at infinity is stationary, the solution represents a vorticity distribution which translates uniformly without change of form toward negative  $x$ . Note, however, that the maximum amplitude of  $\eta_s$  (about 1.6 when multiplied by  $\Gamma_s$  – see Fig. 2) is certainly of sufficient amplitude to call in to question the validity of linear theory which, recall, requires  $\eta \ll 1$ . Given this, the linear solution is at most an indication that a nonlinear (i.e., exact) translating V-state may exist.

Finally, it is noted that the linear V-state has zero net circulation. To see this first note that the area  $A$  of the displaced contour is

$$A = -\frac{\Gamma}{2U\pi} \int_{-\infty}^{\infty} \int_{-\infty}^{\infty} \frac{\operatorname{sgn} k e^{-|k|} \cos(kU\pi)}{k - (\operatorname{sgn} k)/(2U)} e^{ikx} dk dx = -\frac{2\Gamma}{U} \int_0^{\infty} \frac{e^{-|k|} \cos(kU\pi)}{k - 1/(2U)} \delta(k) dk = 2\Gamma. \quad (16)$$

Since the vorticity of the fluid bounded between the displaced contour and the step is  $-1$ , the total circulation of this region is  $-2\Gamma$ . Since there are two line vortices each of strength  $\Gamma$ , it follows that the linear solution has zero total circulation. Crowdy [5] also finds that total circulation vanishes in his exact steady multipolar vortex solutions.

#### 4. Computation of the nonlinear V-state

The numerical procedure of McDonald [12] is used to compute the nonlinear steady solution. Newton's method is used to iterate toward a solution symmetric in  $x$ , which has constant streamfunction along the contour (i.e., the contour becomes

a streamline) and vanishing velocity at each vortex. In so doing the contour shape is computed along with the parameters  $L$ ,  $U$  and  $\Gamma$ . The method requires the computation of velocities along the contour and at both vortices. Owing to the piecewise constant distribution of vorticity, in order to compute these velocities it is appropriate to use a modified version (Dunn et al. [10]) of the efficient contour dynamics algorithm of Dritschel [15].

The non-radiating V-state must be symmetric in  $x$  and this property is ensured by restricting the computational domain to positive values of  $x$ , namely  $0 \leq x \leq W$ , where  $W \gg 1$  and assuming symmetry about  $x = 0$ . The contour is discretized into  $N + 1$  uniformly spaced points  $x_i$ , each with displacement  $y_i$ ,  $i = 1, \dots, N + 1$ . For a given contour displacement the velocity at each point on the contour and at the vortices located at  $(\pm L/2, -1)$  is computed by the contour dynamics algorithm which also takes into account the ambient flow speed  $U$  and the velocity field owing to both vortices. The value of the streamfunction  $\psi_i$  is then computed at each point on the contour marching to the left, beginning at the end point  $\psi_{N+1} = 0$  at  $x = W$ , according to the formula

$$\psi_i = \psi_{i+1} - \bar{v}_i dx_i + \bar{u}_i dy_i, \quad i = 1, \dots, N, \quad (17)$$

where

$$\bar{v}_i = \frac{v(i) + v(i+1)}{2}, \quad \bar{u}_i = \frac{u(i) + u(i+1)}{2}, \quad i = 1, \dots, N, \quad (18a,b)$$

and

$$dx_i = x_{i+1} - x_i, \quad dy_i = y_{i+1} - y_i, \quad i = 1, \dots, N. \quad (19a,b)$$

Steady state is achieved by simultaneously adjusting  $y_i$ ,  $\Gamma$ ,  $U$  and  $L$  so that  $\psi_i = 0$ ,  $i = 1, \dots, N + 1$  (i.e., the contour becomes a streamline) and, further, demanding that the velocity field at the vortex at  $(L/2, -1)$  vanishes (symmetry ensures that the velocity vanish at the other vortex). By fixing the last two points in the computational domain  $y_N$  and  $y_{N+1}$ , the  $N + 2$  unknowns  $y_i$  ( $i = 1, \dots, N - 1$ ),  $\Gamma$ ,  $U$  and  $L$  are sought such that they satisfy the  $N + 2$  equations

$$\begin{aligned} \psi_i(y_1, y_2, \dots, y_{N-1}, \Gamma, U, L) &= 0, \quad i = 1, \dots, N, \\ u_{\text{vort}}(y_1, y_2, \dots, y_{N-1}, \Gamma, U, L) &= 0, \\ v_{\text{vort}}(y_1, y_2, \dots, y_{N-1}, \Gamma, U, L) &= 0, \end{aligned} \quad (20)$$

where  $u_{\text{vort}}$  and  $v_{\text{vort}}$  are the components of the velocity field felt at the vortex at  $(L/2, -1)$ . Fixing the last two points to zero (i.e.,  $y_N = y_{N+1} = 0$ ) on the contour also has the desired effect of eliminating downstream and, in this symmetric configuration, upstream waves.

Eqs. (20) are solved using Newton's method, i.e., given the  $n$ -th iteration, the  $(n + 1)$ -th iteration is computed according to

$$\begin{aligned} y_j^{(n+1)} &= y_j^{(n)} + \Delta_j, \quad j = 1, \dots, N - 1, \\ \Gamma^{(n+1)} &= \Gamma^{(n)} + \Delta_N, \\ U^{(n+1)} &= U^{(n)} + \Delta_{N+1}, \\ L^{(n+1)} &= L^{(n)} + \Delta_{N+2}, \end{aligned} \quad (21)$$

where  $\Delta_j$  is the  $j$ -th element of the vector solution of the  $(N + 2) \times (N + 2)$  matrix equation

$$\begin{aligned} \sum_{j=1}^{N-1} \frac{\partial \psi_i^{(n)}}{\partial y_j} \Delta_j + \frac{\partial \psi_i^{(n)}}{\partial \Gamma} \Delta_N + \frac{\partial \psi_i^{(n)}}{\partial U} \Delta_{N+1} + \frac{\partial \psi_i^{(n)}}{\partial L} \Delta_{N+2} &= -\psi_i^{(n)}, \quad i = 1, \dots, N, \\ \sum_{j=1}^{N-1} \frac{\partial u_{\text{vort}}^{(n)}}{\partial y_j} \Delta_j + \frac{\partial u_{\text{vort}}^{(n)}}{\partial \Gamma} \Delta_N + \frac{\partial u_{\text{vort}}^{(n)}}{\partial U} \Delta_{N+1} + \frac{\partial u_{\text{vort}}^{(n)}}{\partial L} \Delta_{N+2} &= -u_{\text{vort}}^{(n)}, \\ \sum_{j=1}^{N-1} \frac{\partial v_{\text{vort}}^{(n)}}{\partial y_j} \Delta_j + \frac{\partial v_{\text{vort}}^{(n)}}{\partial \Gamma} \Delta_N + \frac{\partial v_{\text{vort}}^{(n)}}{\partial U} \Delta_{N+1} + \frac{\partial v_{\text{vort}}^{(n)}}{\partial L} \Delta_{N+2} &= -v_{\text{vort}}^{(n)}. \end{aligned} \quad (22)$$

As in McDonald [12] the derivatives in the above matrix are approximated numerically according to

$$\frac{\partial f}{\partial z} \approx \frac{f(z + \delta) - f(z)}{\delta}, \quad (23)$$

using  $\delta = 10^{-6}$ . Thus to calculate each column  $j$  of the matrix, a small displacement  $\delta$  given to  $y_j$  (or  $\Gamma$ ,  $U$  or  $L$  for the final three columns), the contour dynamics algorithm is then called in order to calculate the velocities at points  $i = 1, \dots, N$  so that

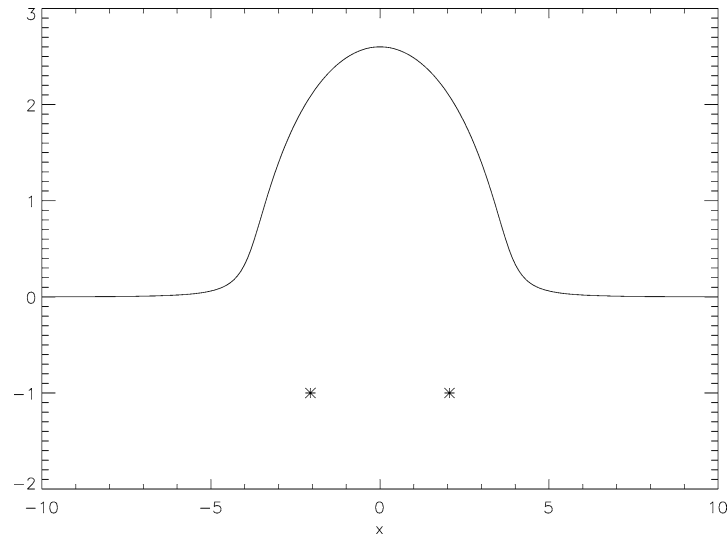


Fig. 4. The nonlinear V-state profile of  $\eta(x)$  and the location of the line vortices (indicated by the stars).

the new streamfunction  $\psi_i(y_j + \delta)$  at points  $i = 1, \dots, N$  can be evaluated. Note that the contour dynamics algorithm is not used here in its usual time-dependent form (Dritschel [15]), but rather it is used only to find the velocities at points along the contour (so that the streamfunction at such points can be calculated) and the vortices and is not used to advect these points. Finally, the matrix equation (22) is solved by Gaussian elimination. Each iteration therefore requires  $N + 3$  calculations for the velocity field at all points, so that the contour dynamics cost is  $(N + 3) \times (N + 3)$ . In addition, at each iteration a  $(N + 2) \times (N + 2)$  matrix inversion is performed. Convergence is monitored by computing the values of  $u_{\text{vort}}$  and  $v_{\text{vort}}$  and the area bounded by the contour and  $y = 0$  at each iteration.

The numerical parameters chosen are  $N = 400$ ,  $0 \leq x \leq 20$  giving a resolution of  $\Delta x = 0.05$  in the  $x$ -direction. Increasing the resolution along the contour, does not affect any of the results to the quoted degree of accuracy, nor does increasing the length of domain. As will be seen, this latter effect is owing to the rapid decay of  $\eta(x)$  for the computed V-state as  $x \rightarrow \infty$ . The results are also insensitive to the choice of  $\delta$ , provided it is sufficiently small.

A variety of initial conditions were tried in order to achieve convergence, including the linear V-state of the previous section. Trial and error showed that convergence is achieved when starting from an initial profile given by  $\eta(x) = 2.5 \exp[-(x/2\pi U_0)^2]$  where the initial speed  $U_0 = 0.64$ ,  $L_0 = 2\pi U_0$  and  $\Gamma_0 = 8.0$ . After 20 iterations the quantities  $\Gamma$ ,  $U$  and  $L$  had converged to 3 significant figures. In particular, it is found that  $\Gamma = 7.74$ ,  $U = 0.641$  and  $L = 4.12$ . Further, the velocity in the  $y$ -direction at each vortex has magnitude of the order  $10^{-8}$ . Further iteration shows that the velocity in the  $y$ -direction becomes even smaller, albeit relatively slowly. Note that the value of  $2\pi U/L = 0.978$  for the nonlinear numerically computed V-state which is close to the value of unity predicted by linear theory (though there is no reason why the nonlinear solution should have unit value for this ratio). A plot of the numerically computed V-state showing the contour displacement and the location of the line vortices is shown in Fig. 4. An immediate feature to note is the rapid decay of  $\eta(x)$  beyond  $|x| \approx 5$ . This explains the insensitivity of the numerical results to the width of the computational domain (provided it is larger than, say, about 10 units). Note also the maximum amplitude of  $\eta(x)$  is twice that of the distance of the vortices from the step, implying that the structure is highly nonlinear. Another feature is that the area bounded by  $y = \eta(x)$  and  $y = 0$  is computed numerically to be 15.5 (to three significant figures) which is approximately equal to twice the circulation of the V-state vortices (i.e.,  $2\Gamma = 15.48$ ). Thus the nonlinear V-state is very close to having zero net circulation. This result may have been expected on the basis of the linear solution of Section 3. Note that the zero net circulation condition arises ‘naturally’; that is, it is not forced by the algorithm.

## 5. Nonlinear evolution of the V-state

The lack of analytic expressions for the nonlinear V-state inhibits (but does not preclude) an investigation of the linear stability of the V-state. Instead, here, the stability or ‘robustness’ of the computed V-state is tested by using it as the initial condition in a fully nonlinear, time-dependent contour dynamics simulation. If the nonlinear V-state is stable then it should remain unchanged for many vortex turnover times. On the other hand, if it is unstable it will rapidly lose coherence and behave in a complicated manner.



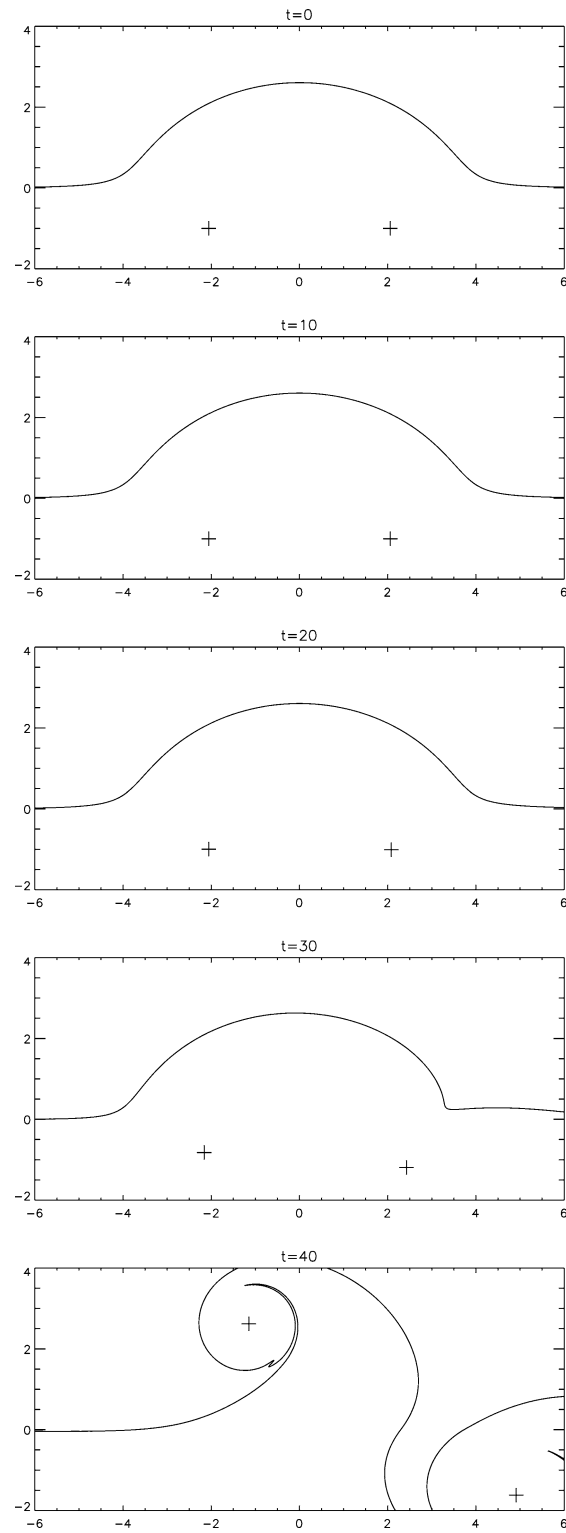


Fig. 5. Evolution of the V-state.

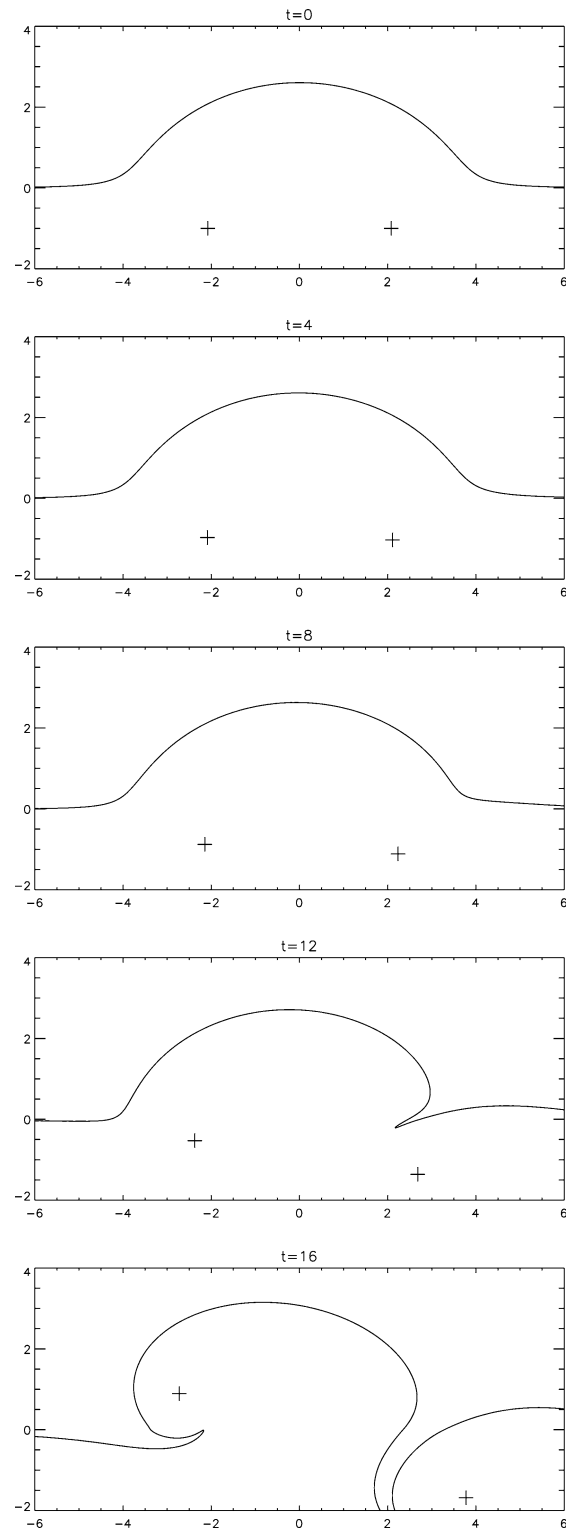


Fig. 6. Evolution of the perturbed V-state. In comparison to Fig. 5, the initial vortex separation has been increased by one percent.

The time-dependent contour dynamics routine is run using the same resolution as used in the V-state computation of the previous section in a domain of width 40 units. In the time-dependent routine the velocity field is calculated at nodes along the contour as well as each vortex and is used to advect the nodes and the vortices. A 4th order Runge–Kutta routine is used for the time-stepping. Fig. 5 shows the evolution of the V-state. Note that up to time  $t = 20$  the V-state remains visibly unchanged. The vortex turnover time at unit distance from a vortex is about 5 time units and hence the V-state is able to survive about 4 turnover times during which it travels a distance of about 13 units which is approximately three times the initial separation distance of the two line vortices. For times beyond  $t = 20$  the V-state begins to lose its coherence. Fig. 5 shows that at  $t = 30$  the interface profile becomes asymmetric and the vortices are no longer the same distance from the step. The V-state then rapidly breaks up and evolves in a complicated manner ( $t = 40$ ).

For comparison, Fig. 6 shows the same experiment but with the V-state perturbed so that the initial distance between the vortices is increased by one percent. Not unexpectedly, the break-up of the initial state is more rapid, with evidence for asymmetry developing in the interface profile observable after  $t = 8$ . Beyond  $t = 12$  the initial configuration has lost all coherence and evolves in a complicated manner. In this case the initial configuration is unable to propagate much farther than a distance equal to the initial separation of the two vortices before breaking up.

While it is difficult to be conclusive, the time-dependent simulations suggest that the V-state is unstable, with a small perturbation in the vortex separation distance leading to relatively rapid break-up. However, the growth rate of disturbances of the unperturbed V-state is relatively small and the V-state is able to propagate coherently over a distance equal to several times its own lengthscale.

## 6. Conclusion

It is well-known that geophysical vortices have a natural tendency to self-propagate with regions of low potential vorticity on their right. On a rotating earth this is manifested as a westward propagation. As they do so, they radiate waves, these being, for example, Rossby waves on a rotating earth, or in the case of the present work, topographic waves. The wave radiation implies that generally geophysical vortices must propagate unsteadily. On a  $\beta$ -plane and using linear quasigeostrophic theory, McDonald and Johnson [16] found that two vortices could be arranged such that the energy radiated of Rossby waves could be minimised, but never made to vanish owing to the two-dimensional nature of the radiated Rossby wave field. In contrast, the one-dimensional wave guide of the present work enables the placement of two wave making objects, in this case vortices, such that, according to linear theory at least, their wakes precisely cancel each other so that there is no net drag on the pair. This was shown to be the case in Section 2, where it was further demonstrated that there existed a unique choice of vortex circulation  $\Gamma_s$  and vortex separation  $L_s$  such that the vortices self-propagate steadily with speed  $U_s$ . While the linear theory of Section 2 is encouraging in that it demonstrates the existence of linear V-state, it is in a sense ‘self-destructive’ since it predicts an amplitude of the contour displacement way beyond the validity of linear theory. This motivated the successful search for a nonlinear V-state using numerical methods. It is, of course, possible for Newton’s method to miss possible solutions, however an extensive (but not exhaustive) search of parameter space revealed no other converged V-state solutions.

Time-dependent contour dynamics simulations suggest the V-state is unstable, although the growth rate of unstable disturbances is small enabling it to propagate a significant distance before disintegrating. Nevertheless, the solution suggests that other translating V-states of the type found here perhaps involving more than two vortices are possible and, if so, some of these may be stable.

It would be of interest to see if translating V-states of the type found here could be derived analytically. The analytical methods employed by Crowdy [5–7] in finding rotating V-states may be of use in this respect, especially when it realised that, like the V-state found here, Crowdy’s V-states also involve a combination of finite-area patches of constant vorticity and line vortices with zero total circulation. It would also be of interest, especially in the oceanographic context, to introduce a free-surface to the physical problem. In this quasigeostrophic formulation, this introduces an extra parameter namely the radius of deformation and would, possibly, generate a one parameter family of solutions some of which may be stable. Finally (as suggested by a referee) it may be possible to find propagating V-state solutions comprising of oppositely signed vortices located on either side of the step and an interface profile which is antisymmetric.

## Acknowledgement

I am grateful for comments made by the referees which have helped to improve this paper.

## References

- [1] H. Aref, P.K. Newton, M.A. Stremler, T. Tokieda, D.L. Vainchtein, Vortex crystals, *Adv. Appl. Mech.* 39 (2002).
- [2] G.S. Deem, N.J. Zabusky, Stationary ‘V-states’, interactions, recurrence and breaking, *Phys. Rev. Lett.* 40 (1978) 859–862.
- [3] H.M. Wu, E.A. Overman, N.J. Zabusky, Steady state solutions of the Euler equations in two dimensions. Rotating and translating V-states with limiting cases, *J. Comput. Phys.* 53 (1984) 42–71.
- [4] R.T. Pierrehumbert, A family of steady, translating vortex pairs with distributed vorticity, *J. Fluid Mech.* 99 (1980) 129–144.
- [5] D.G. Crowdy, A class of exact multipolar vortices, *Phys. Fluids* 11 (1999) 2556–2564.
- [6] D.G. Crowdy, The construction of exact multipolar equilibria of the two-dimensional Euler equations, *Phys. Fluids* 14 (2002) 257–267.
- [7] D.G. Crowdy, Exact solutions for rotating vortex arrays with finite-area cores, *J. Fluid Mech.* 469 (2002) 209–235.
- [8] V.V. Meleshko, G.J.F. van Heijst, On Chaplygin’s investigations of two-dimensional vortex structures in an inviscid fluid, *J. Fluid Mech.* 272 (1994) 157–182.
- [9] G.R. Flierl, V.D. Larichev, J.C. McWilliams, G.M. Reznik, The dynamics of baroclinic and barotropic solitary eddies, *Dyn. Atmos. Oceans* 5 (1980) 1–41.
- [10] D.C. Dunn, N.R. McDonald, E.R. Johnson, The motion of a singular vortex near an escarpment, *J. Fluid Mech.* 448 (2001) 335–365.
- [11] G.I. Bell, Interaction between vortices and waves in a simple model of geophysical flow, *Phys. Fluids A* 2 (1990) 575–586.
- [12] N.R. McDonald, Steady, nonradiating geophysical flow past a cylinder with circulation, *Phys. Fluids* 14 (2002) 3018–3027.
- [13] E.O. Tuck, D.C. Scullen, Tandem submerged cylinders each subject to zero drag, *J. Fluid Mech.* 364 (1998) 211–220.
- [14] N.R. McDonald, The motion of an intense vortex near topography, *J. Fluid Mech.* 367 (1998) 359–377.
- [15] D.G. Dritschel, Contour dynamics and contour surgery: numerical algorithms for extended, high resolution modelling of vortex dynamics in two-dimensional, inviscid, incompressible flows, *Comp. Phys. Rep.* 10 (1989) 77–146.
- [16] N.R. McDonald, E.R. Johnson, The interaction of two vortices on a beta-plane, *Phys. Fluids* 13 (2001) 884–893.